JOURNAL OF COMPUTATIONAL PHYSICS 37, 41–55 (1980)

A Fourier Bessel Transform Method for Efficiently Calculating the Magnetic Field of Solenoids*

JACK NACHAMKIN† AND C. J. MAGGIORE

Los Alamos Scientific Laboratory, Los Alamos, New Mexico

Received June 19, 1978; received May 22, 1979

A numerical procedure for calculating the magnetic field of a solenoid is derived. Based on the properties of Bessel functions, the procedure is shown to be convergent everywhere, including within the windings of the solenoid. The most critical part of the procedure is detailed in the main text. A simple method is used to ensure numerical significance while allowing economical computational times. In the appendix the procedure is generalized to universal convergence by appropriate partitioning of the solenoid windings.

I. INTRODUCTION

Any method of accurately calculating charged particle trajectories in solenoidal magnetic fields requires a knowledge of the magnetic field at every point along the path. The usual methods of calculating a magnetic field [1–5] are not well suited to the problem if a trajectory both inside and outside the magnet and far from the axis of the solenoid is required. Some methods also have difficulty if the solenoid is thin, or high accuracy is required. The following method based on the properties of Bessel functions and Fourier Bessel transforms has characteristics that make it well suited to the problem. The same algorithm can be used to calculate the magnetic field everywhere without having to transform the origin. The resultant series expansion in r, the distance from the axis, converges rapidly, and the method is easily programmed. There are no restrictions on the allowable aspect ratio of the magnet.

Using this technique, a numerical procedure was evolved having a wide variety of applications. The main body of this paper deals with deriving the fundamental formulas applied to generating a series in positive powers of r. A variation of the method, producing a convergent series in negative powers of r, is introduced in such a way as to yield a procedure that converges everywhere, even within the windings of the solenoid.

This work was performed under the auspices of the U.S. Department of Energy.

† Present address: Exxon Enterprises, Inc., Sunnyvale, CA.

0021-9991/80/100041-15$02.00/0

II. Mathematical Theory

A magnetic field, **B**, in a current-free medium can be derived from a scalar potential, ϕ. Thus,

$$\mathbf{B} = -\nabla\phi \tag{1}$$

and

$$\nabla^2\phi = 0. \tag{2}$$

Equation (2) can be solved for ϕ if ϕ is specified on some boundary. As an important case, the apparent magnetic potential of a circular loop of current can be written in the plane of the loop as

$$\begin{aligned} \phi &= \tfrac{1}{2}I\mu_0 \quad \text{if} \quad r < R \text{ viewed from } z > 0, \\ &= -\tfrac{1}{2}I\mu_0 \quad \text{if} \quad r < R \text{ viewed from } z < 0, \\ &= 0 \quad \text{if} \quad r > R, \end{aligned} \tag{3}$$

where I is the circulating current, μ_0 is the permeability of the medium, R is the radius of the loop, and r is the distance from the center of the loop.

Because of cylindrical symmetry, ϕ can be expressed everywhere for $z \gtrless 0$, except at the radius of the loop, as the Bessel transform [6]

$$\phi(r, z) = \int_0^\infty A(\lambda, R)\, J_0(\lambda r) e^{-\lambda z}\, d\lambda, \tag{4}$$

where the origin of the cylindrical coordinates is at the center of the loop. The function $A(\lambda, R)$ depends only on λ, R, μ_0, and the current I.

Using Eq. (3), Eq. (4) can be solved for $A(\lambda, R)$ in the plane of the loop from Bessel transform theory [6]. The resulting potential is

$$\phi(r, z) = \tfrac{1}{2}IR\mu_0 \int_0^\infty J_1(\lambda R)\, J_0(\lambda r) e^{-\lambda z}\, d\lambda. \tag{5}$$

From Eqs. (1) and (3) the components of the field can be found:

$$B_z = -\partial\phi/\partial z = \tfrac{1}{2}IR\mu_0 \int_0^\infty \lambda J_1(\lambda R)\, J_0(\lambda r) e^{-\lambda|z|}\, d\lambda, \tag{6}$$

and

$$B_r = -\partial\phi/\partial r = \operatorname{sgn}(z)\tfrac{1}{2}IR\mu_0 \int_0^\infty \lambda J_1(\lambda R)\, J_1(\lambda r) e^{-\lambda|z|}\, d\lambda, \tag{7}$$

where $\operatorname{sgn}(z) = \pm 1$ for $z \gtrless 0$. The function $\operatorname{sgn}(z)$ determines the sense of a positive current, counterclockwise or clockwise, when viewed from $z > 0$.

The field of an axially symmetric solenoid can be derived as a superposition of loop fields given in (6) and (7). Given a solenoid with rectangular cross section, inner radius R_1, outer radius R_2, and width $2z_0$, let the origin of a cylindrical coordinate system be at the geometrical center of the coil with the z axis aligned with the axis of the solenoid. It will further be assumed that the current in the solenoid is distributed evenly throughout its cross section. Equations (6) and (7) can then be integrated over the cross section to give the field for $|z| < z_0$:

$$B_z = I\mu_0 \int_{R_1}^{R_2} RdR \int_0^\infty J_1(\lambda R)\, J_0(\lambda r)\, [1 - e^{-\lambda z_0} \cosh \lambda z]\, d\lambda \tag{8}$$

and

$$B_r = I\mu_0 \int_{R_1}^{R_2} RdR \int_0^\infty J_1(\lambda R)\, J_1(\lambda r) e^{-\lambda z_0} \sinh \lambda z\, d\lambda. \tag{9}$$

For $|z| > z_0$,

$$B_z = I\mu_0 \int_{R_1}^{R_2} RdR \int_0^\infty J_1(\lambda R)\, J_0(\lambda r) e^{-\lambda |z|} \sinh \lambda z_0\, d\lambda \tag{10}$$

and

$$B_r = I\mu_0 \int_{R_1}^{R_2} RdR \int_0^\infty J_1(\lambda R)\, J_1(\lambda r) e^{-\lambda |z|} \sinh \lambda z_0 \operatorname{sgn}(z)\, d\lambda, \tag{11}$$

where I is now the current *density* in the solenoid's cross section.

Numerically Eqs. (8)–(11) present two main cases for integration:

$$S_{10}(r, z) = \int_{R_1}^{R_2} RdR \int_0^\infty J_1(\lambda R)\, J_1(\lambda r) e^{-\lambda z}\, d\lambda \tag{12}$$

and

$$S_{11}(r, z) = \int_{R_1}^{R_2} RdR \int_0^\infty J_1(\lambda R)\, J_1(\lambda r) e^{-\lambda z}\, d\lambda. \tag{13}$$

By allowing z_0 to become very large in Eq. (8), it can immediately be deduced that

$$\begin{aligned} \bar{S}_{10}(r) &= \int_{R_1}^{R_2} RdR \int_0^\infty J_1(\lambda R)\, J_0(\lambda r)\, d\lambda, \\ &= R_2 - R_1 \qquad \text{if} \quad r < R_1, \\ &= R_2 - r \qquad \text{if} \quad R_1 \leqslant r \leqslant R_2, \\ &= 0 \qquad \text{if} \quad r > R_2, \end{aligned} \tag{14}$$

because as $z_0 \to \infty$ the exponential term in the bracket vanishes. The field in this case becomes a constant where $r < R_1$, equal to $I\mu_0 (R_2 - R_1)$, hence Eq. (14). Equation (14) is a special case of a discontinuous Weber–Schafheitlin integral [7, 8]. The meaning of Eq. (14) is that solutions obtained by the methods outlined below will describe the field of a solenoid everywhere they converge, including inside the windings of the solenoid.

In terms of the S integrals, for $|z| \leqslant z_0$:

$$B_z = I\mu_0 \tilde{S}_{10}(r) - \tfrac{1}{2} I\mu_0 [S_{10}(r, z_0 - z) + S_{10}(r, z_0 + z)] \tag{15}$$

and

$$B_r = \tfrac{1}{2} I\mu_0 [S_{11}(r, z_0 - z) - S_{11}(r, z_0 + z)]. \tag{16}$$

For $|z| > z_0$:

$$B_z = \tfrac{1}{2} I\mu_0 [S_{10}(r, |z| - z_0) - S_{10}(r, |z| + z_0)] \tag{17}$$

and

$$B_r = \tfrac{1}{2} I\mu_0 \operatorname{sgn}(z) [S_{11}(r, |z| - z_0) - S_{11}(r, |z| + z_0)]. \tag{18}$$

III. Calculating the S Integrals

The first method of choice in evaluating $S_{10}(r, z)$ and $S_{11}(r, z)$ was to expand the respective integrands in powers of r. In theory, these power series could be generated from a knowledge of the z derivatives of the field along the axis, which can be written in closed form [9]. Using the properties of Bessel functions, however, greatly simplifies this task.

For example, Eq. (12) can be rewritten by expanding $J_0(\lambda r)$:

$$S_{10}(r, z) = \int_{R_1}^{R_2} R\,dR \sum_{m=0}^{\infty} \frac{(-1)^m r^{2m}}{2^{2m}(m!)^2} \int_0^{\infty} \lambda^{2m} J_1(\lambda R) e^{-\lambda z}\, d\lambda. \tag{19}$$

The λ integral can be evaluated from the general formula [8]

$$\int_0^{\infty} t^n J_k(t \sin\beta) e^{-t\cos\beta}\, dt = \Gamma(n + k + 1)\, P_n^{-k}(\cos\beta), \tag{20}$$

where $\Gamma(\chi)$ is the gamma function and $P_n^{-k}(\chi)$ is the associated Legendre function of the first kind of degree n and order $-k$.

A form for this associated Legendre function with k equal 1 can be found in Sneddon's book [10], referred to as Ferrer's function,

$$P_\mu^{-1}(x) = (1-x^2)^{-1/2} \int_1^x P_\mu(x')\, dx'. \tag{21}$$

Using the power series expansion for Legendre functions [7], one obtains

$$S_{10}(r,z) = \sum_{m=0}^{\infty} \frac{(-1)^m (2m+1)!}{2^{4m+1}(m!)^2} r^{2m} \sum_{k=0}^{m} \frac{(-1)^k \binom{2m}{k} \binom{4m-2k}{2m}}{m+\frac{1}{2}-k}$$

$$\times \int_{R_1}^{R_2} \{[R^2+z^2]^{-m} - z^{2m+1-2k}[R^2+z^2]^{-2m-(1/2)+k}\}\, dR, \tag{22}$$

where

$$\binom{n}{k} = \frac{n!}{k!(n-k)!}. \tag{23}$$

The original Bessel function integrals over the volume of the windings is thus reduced to the sum of the elementary integrals in Eq. (22).

Renaming the integral

$$K_{2m}(z) = \int_{R_1}^{R_2} [R^2+z^2]^{-m}\, dR, \tag{24}$$

the S integrals can be written

$$S_{10}(r,z) = \sum_{m=0}^{\infty} r^{2m} \sum_{k=0}^{m} C_0^{m,k}[K_{2m}(z) - z^{2m+1-2k}K_{4m+1-2k}(z)] \tag{25}$$

and

$$S_{11}(r,z) = \sum_{m=0}^{\infty} r^{2m} \sum_{k=0}^{m} C_1^{m,k}[K_{2m+1}(z) - z^{2m+2-2k}K_{4m+3-2k}(z)], \tag{26}$$

where

$$C_0^{m,k} = \frac{(-1)^{m+k}(2m+1)! \binom{2m}{k} \binom{4m-2k}{2m}}{2^{4m+1}(m!)^2(m+\frac{1}{2}-k)} \tag{27}$$

and

$$C_1^{m,k} = \frac{(-1)^{m+k}(2m+2)! \binom{2m+1}{k} \binom{4m+2-2k}{2m+1}}{2^{4m+3}m!(m+1)!\,(m+1-k)}. \tag{28}$$

The C coefficients are independent of r and z and need only be calculated once. The values of the $K_m(z)$'s may be found as follows: The substitution

$$R = z \tan \theta \tag{29}$$

in Eq. (24) reduces it to the form

$$K_{2m}(z) = z^{1-2m} \int_{\theta_1}^{\theta_2} (\cos \theta)^{2m-2}\, d\theta. \tag{30}$$

Knowing $K_{2m}(z)$ for $m = 0, -\frac{1}{2}, 1$, and $-\frac{3}{2}$, it is possible to determine all the $K_{2m}(z)$'s by forward recursions, i.e., using the relation,

$$\int \cos^n \chi d\chi = \frac{1}{n} \cos^{n-1} \chi \sin \chi + \frac{n-1}{n} \int \cos^{n-2} \chi d\chi. \tag{31}$$

For small values of z the use of (31) introduces inaccuracies due to loss of significance. A value of z must then be chosen, below which forward recursion cannot be relied upon for a given numerical significance. Instead, the integral in Eq. (30) can be expanded as an ascending power series in $\cos \theta$ to any desired accuracy using Eq. (31):

$$\int (\cos \theta)^m\, d\theta = -\sin \theta\, (\cos \theta)^{m+1} \left[\frac{1}{m+1} + \frac{m+2}{m+1} \frac{\cos^2 \theta}{m+3} + \cdots \right]. \tag{32}$$

It is easy to see that Eq. (32) will not converge very quickly if

$$\cos \theta \approx 1. \tag{33}$$

It is therefore not economical to use the expansion in (32) every time just to avoid forward recursions in Eq. (31).

Experience using the above procedure showed that, for a given set of solenoid dimensions, a crossover value z_c could be chosen. For $z > z_c$ forward recursion using (31) was performed with 25-digit accuracy. For $z \leqslant z_c$, Eq. (32) was used. To estimate the extent of the loss of significance for small values of z in forward recursion suppose

$$z = z_c. \tag{34}$$

Then define

$$A_{m+2} \equiv \int_{\theta_1}^{\theta_2} \cos^{m+2} \theta d\theta = \int_{R_1}^{R_2} \frac{z_c^{m+2}\, dR}{[R^2 + z_c^2]^{(1/2)m+1}}, \tag{35}$$

so that

$$(z_c/R_1)^2 A_m > A_{m+2} > (z_c/R_2)^2 A_m. \tag{36}$$

The number of significant decimal digits, N, lost per forward iteration evidently satisfies

$$-2\log(z_c/R_1) < N < -2\log(z_c/R_2). \tag{36a}$$

Care must then be taken such that at the end of a sequence of forward recursions there is enough significance left to give an accurate answer. In the next section a technique will be described that reliably calculates magnetic fields of solenoids taking these numerical constraints into account.

IV. Numerical Procedure

The most difficult task encountered in implementing the above theory was to avoid loss of significant digits as a result of recursions and cancellation of large numbers. Convergence of the power series expansions for $S_{10}(r, z)$ and $S_{11}(r, z)$ is discussed in the appendix, where it is shown that there are two overlapping regions of convergence corresponding to two different methods of expanding the integrals. The method below converges in the region including the entire axis of the solenoid and in fact converges for some $r > R_1$ beyond the ends of the solenoid where R_1 is the inner radius of the solenoid.

When discussing the relative merits of using Eqs. (31) and (32), it was mentioned that a crossover point was chosen so that if $z \geqslant z_c$, Eq. (31) was implemented using double precision (25 digits). If $z < z_c$, Eq. (32) was used with single precision. A satisfactory value for z_c was found to be

$$z_c = \tfrac{1}{2}R_1. \tag{37}$$

A maximum of 40 terms is retained in the square bracket in Eq. (32). The highest power of r retained in S_{10} is r^{18}. The highest in S_{11} is r^{19}.

Equations (27) and (28) were not used directly to derive the C's because of possible overflow problems. Instead the following set of recursions was used:

$$C_1^{0,0} = \tfrac{1}{2}, \tag{38a}$$

$$C_0^{0,0} = 1, \tag{38b}$$

$$C_0^{m,k} = -\frac{(m-k+1)(2m-2k+1)(m+\frac{3}{2}-k)}{k(4m-2k+1)(m+\frac{1}{2}-k)}\, C_0^{m,k-1}, \tag{38c}$$

and

$$C_1^{m,k} = \frac{(4m+1-2k)(m+\frac{1}{2}-k)}{(2m+1-2k)(m+1-k)}\, C_0^{m,k}.$$

and

$$C_1^{m,k} = \frac{(4m+1-2k)(m+\frac{1}{2}-k)}{(2m+1-2k)(m+1-k)} C_0^{m,k}. \tag{38d}$$

Using the integral [7]

$$\int_0^\infty t^\mu J_\nu(t)\, dt = 2^\mu \Gamma\left(\frac{\nu+\mu+1}{2}\right) \Big/ \Gamma\left(\frac{\nu-\mu+1}{2}\right), \tag{39}$$

it can be shown that

$$\sum_{k=0}^{m} C_0^{m,k} = \delta_{m,0}\delta_{k,0}. \tag{40}$$

This means that the term $K_{2m}(z)$ with $m \neq 0$ in Eq. (25) does not contribute to the sum and can be eliminated. Doing so makes very little difference in the final result for most values of z. Equation (40) serves as a valuable check on the calculation of the C's. A more involved analysis can be applied to the $C_1^{m,k}$s. To the accuracy we needed, it made no difference when the $C_1^{m,k}$ sum on k was replaced. Convergence to at least six significant figures was always possible with 19 powers of r for $r \leqslant R_1$.

As an example, a solenoid with

$$R_1 = 2.5 \text{ cm}, \tag{41a}$$

$$R_2 = 16.0 \text{ cm}, \tag{41b}$$

and

$$z_0 = 2.5 \text{ cm} \tag{41c}$$

was calculated. The current density was taken to be 1.3×10^4 A/cm^2. At the center of the solenoid the z component of the magnetic field was

$$B_z = 6.83722 \text{ Tesla}. \tag{42}$$

Tables I, II, and III show the convergence of the magnetic field at points 2.5 cm from the axis. Convergence further from the axis is discussed in the appendix. The z coordinate is measured from the center of the solenoid. Depending on the distance from the edges of the solenoid and the distance from the axis, convergence can take from under 1 msec to approximately 5 msec on a CDC 7600.

V. Discussion

The theory outlined in the previous sections turns out to be a straightforward numerical procedure. Because of the potential for loss of significance, care must be

TABLE I

$R_1 = 2.5$ cm, $r_2 = 16$ cm, $I = 1.3 \times 10^4$ A/cm^2, $(r, z) = (2.5, 0)$ cm

Highest power of r	B_r (Tesla)	B_z (Tesla)
1	0.0	6.83722
3	0.0	7.64610
5	0.0	7.49653
7	0.0	7.48513
9	0.0	7.48348
11	0.0	7.48446
13	0.0	7.48461
15	0.0	7.48449
17	0.0	7.48447
19	0.0	7.48449
21	0.0	7.48449

TABLE II

$R_1 = 2.5$ cm, $R_2 = 16$ cm, $I = 1.3 \times 10^4$ A/cm^2, $z_0 = 2.5$ cm, $(r, z) = (2.5, 2.5)$ cm

Highest power of r	B_r (Tesla)	B_z (Tesla)
1	0.9851928	5.712192
3	1.010640	5.911321
5	1.010519	5.908042
7	1.010537	5.907809
9	1.010536	5.907865
11	1.010536	5.907859
13	1.010536	5.907859

TABLE III

$R_1 = 2.5$ cm, $R_2 = 16$ cm, $I = 1.3 \times 10^4$ A/cm^2, $z_0 = 2.5$ cm, $(r, z) = (2.5, 5.0)$ cm

Highest power of r	B_r (Tesla)	B_z (Tesla)
1	0.8251600	3.775101
3	0.8206319	3.584169
5	0.8078811	3.564366
7	0.8087418	3.570087
9	0.8096119	3.570912
11	0.8095179	3.570430
13	0.8094174	3.570348
15	0.8094305	3.570408
17	0.8094449	3.570419
19	0.8094428	3.570410

taken if its use is extended into regions with large values of r. The trouble is due in part to the need for precise evaluation of integrals, such as those found in Eq. (36), for small values of z. This defect can be circumvented, however, by choosing the appropriate recursion relations in the direction of higher accuracy.

Another factor affects the accuracy of these calculated integrals. For large values of r the magnetic field is small but the first few terms of the power series can be very large. Thus, a loss of significance is incurred as these large numbers are summed. Since the above expansion was not used in this region, it was not judged economical to generate a more accurate algorithm for the integrals. In the appendix a method is developed that extends the region of stable convergence by summing series of negative powers of r.

Experimentation with the method detailed above shows that convergence improves

TABLE IV

$R_1 = 2.5$ cm, $R_2 = 16$ cm, $I = 1.3 \times 10^4$ A/cm^2,
$z_0 = 2.5$ cm, $(r, z) = (5.0, 7.5)$ cm

Highest power of r	B_r (Tesla)	B_z (Tesla)
1	1.011484	2.468339
3	0.8761310	1.975846
5	0.8725797	2.010794
7	0.8887247	2.026500
9	0.8791547	2.012162
11	0.8815285	2.018027
13	0.8827050	2.017900
15	0.8810454	2.016149
17	0.8818667	2.017492
19	0.881883	2.017130

TABLE V

$R_1 = 2.5$ cm, $R_2 = 16$ cm, $I = 1.3 \times 10^4$ A/cm^2,
$z_0 = 2.5$ cm, $(r, z) = (16, 22.5)$ cm

Highest power of r	B_r (Tesla)	B_z (Tesla)
1	0.2868293	0.3388440
3	0.09284060	0.03210549
5	0.1657673	0.1710878
7	0.1472648	0.1299535
9	0.1511418	0.1388841
11	0.1499722	0.1368353
13	0.1504776	0.1376258
15	0.1503227	0.1373119
17	0.1503218	0.1373698
19	0.1503598	0.1373990

as the distance from either end of the solenoid increases. Using the example of the previous section, Table IV shows the convergence at a point with $r = 5$ cm (twice the inner radius) at 7.5 cm from the center of the solenoid. Table V shows the convergence at $r = 16.0$ cm, 22.5 cm from the center. An exact relation for the regions of convergence is derived in the appendix.

In short, the numerical technique described above is easy to program, fast running on a digital computer, capable of delivering high accuracy, and flexible enough to compute a large range of particle trajectories, parts of which lie at an appreciable distance from the axis.

APPENDIX: Convergence of Series for S_{10} and S_{11}

Using Eq. (20), Eq. (19) may be written

$$S_{10}(r, z) = \sum_{m=0}^{\infty} \frac{(-1)^m r^{2m}(2m+1)!}{2^{2m}(m!)^2} \int_{R_1}^{R_2} R(R^2+z^2)^{-m-1/2} P_{2m}^{-1}\left(\frac{z}{(R^2+z^2)^{1/2}}\right) dR. \tag{A1}$$

In order to study the convergence of the sum in (A1), it is necessary to know the behavior of the integral for large values of m. Using the transformation in Eq. (29), the integral in (A1) becomes

$$H_m = z^{-2m+1} \int_{\theta_1}^{\theta_2} \sin\theta(\cos\theta)^{2m-2} P_{2m}^{-1}(\cos\theta)\, d\theta. \tag{A2}$$

As $m \to \infty$, the asymptotic form [7] of $P_{2m}^{-1}(\cos\theta)$ can be used to give

$$H_m \sim z^{-2m+1} \frac{\Gamma(2m)}{\Gamma(2m+\frac{3}{2})} \left(\frac{1}{2}\pi\right)^2 \times \int_{\theta_1}^{\theta_2} (\sin\theta)^{1/2} (\cos\theta)^{2m-2} \cos\left[\left(2m+\frac{1}{2}\right)\theta - \frac{3\pi}{4}\right] d\theta, \tag{A3}$$

where the gamma function, $\Gamma(\chi)$, has been introduced. From the mean value theorem a $\bar{\theta}$ can be found such that

$$\theta_1 \leqslant \bar{\theta} \leqslant \theta_2 \tag{A4}$$

and

$$H_m \sim z^{-2m+1} \frac{\Gamma(2m)}{\Gamma(2m+\frac{3}{2})} \left(\frac{1}{2}\pi\right)^{-1/2} (\theta_2 - \theta_1)(\sin\bar{\theta})1/2 \times (\cos\bar{\theta})^{2m-2} \cos\left[\left(2m+\frac{1}{2}\right)\bar{\theta} - \frac{3\pi}{4}\right]. \tag{A5}$$

It is evident that H_m is finite for all values of z. This need only be proved for the case $z = 0$. From Eq. (29),

$$\cos\theta = z[R^2 + z^2]^{-1/2}. \tag{A6}$$

Thus as $z \to 0$,

$$\cos\tilde{\theta} < z/R_1. \tag{A7}$$

Expanding the bracketed term in (A6) in powers of $(z/R)^2$ yields the limiting value as $z \to 0$,

$$\theta_2 - \theta_1 \sim z(R_2^{-1} - R_1^{-1}). \tag{A8}$$

Thus as $z \to 0$,

$$|H_m| < \frac{\Gamma(2m)}{\Gamma(2m + \frac{3}{2})} \left(\frac{1}{2}\pi\right)^{-1/2} (R_1^{-1} - R_2^{-1}) R_1^{-2m+2}. \tag{A9}$$

For large values of m Stirling's approximation can be used to show that as $z \to 0$

$$|H_m| < (\tfrac{1}{2}\pi)^{-1/2} R_1^{-2m+1} (2m + \tfrac{3}{2})^{-1/2}. \tag{A10}$$

Equation (A6) may now be substituted into (A5) for all values of $z \neq 0$ with assurance that the resultant analysis will be valid for $z = 0$:

$$H_m \sim (\tfrac{1}{2}\pi)^{-1/2} (2m + \tfrac{3}{2})^{-3/2} [(\theta_2 - \theta_1) z^{-1}] \tilde{R}[\tilde{R}^2 + z^2]^{-(1/2)(2m-3)}, \tag{A11}$$

where $\tilde{R}$ is defined by

$$\cos\tilde{\theta} = z[\tilde{R}^2 + z^2]^{-1/2}. \tag{A12}$$

As $m \to \infty$ it is not difficult to see that

$$\tilde{R} \to R_1. \tag{A13}$$

This is because the largest value of $\cos\theta$ in (A3) is at $R = R_1$.

Replacing the integral in Eq. (A1) with the asymptotic expression for H_m, it is evident that the series for $S_{10}(r, z)$ will converge if

$$r \leqslant [R_1^2 + z^2]^{1/2}. \tag{A14}$$

A similar analysis yields the same radius of convergence for $S_{11}(r, z)$.

In Eq. (A14), as well as Eqs. (12) and (13) of the text, z is measured from the *ends* of the solenoid. Geometrically this means that the region of convergence in an (r, z) plane will lie below the upper limbs of the hyperbolae

$$r^2 - z^2 = R_1^2, \tag{A15}$$

centered at the ends of the solenoid and above the z axis. Even though this is already a large and useful region of convergence, it can be extended to cover the entire (r, z) plane.

To see this it is necessary to go back to Eqs. (12) and (13). Instead of expanding $J_\nu(\lambda r)$'s in ascending power series of (λr), the Bessel function $J_1(\lambda R)$ is expanded:

$$S_{1\nu}(r, z) = \sum_{m=0}^{\infty} \int_{R_1}^{R_2} \frac{(-1)^m R^{2m+2}\, dR}{2^{2m+1} m!(m+1)!} \int_0^{\infty} \lambda^{2m+1} J_\nu(\lambda r) e^{-\lambda|z|}\, d\lambda, \tag{A16}$$

where $\nu = 0, 1$. The integrals in (A16) can be evaluated using Eq. (20) so that

$$S_{1\nu}(r, z) = \sum_{m=0}^{\infty} \frac{(-1)^m (R_2^{2m+3} - R_1^{2m+3})\,(2m+\nu+1)!}{2^{2m+1}(2m+3)\, m!(m+1)!} \times [r^2 + z^2]^{-(m+1)} P_{2m+1}^{-\nu}\left(\frac{z}{(r^2+z^2)^{1/2}}\right). \tag{A17}$$

By substituting the asymptotic expression [7] for $P_{2m+1}^{-\nu}(\chi)$, as $m \to \infty$, into (A17), as well as using Stirling's approximation to evaluate the factorials, it is easy to show that (A17) converges if

$$r^2 + z^2 \geqslant R_2^2. \tag{A18}$$

Note that (A17) has powers of r in the denominator of each term, but is not an asymptotic series. In constrast with the terms in (A1) the terms in (A17) can be evaluated with little loss of significance, except at zeros on the interval $-1 < \chi < 1$, by the forward recursion relation [7]

$$P_{n+1}^{-\nu}(\chi) = [(2n+1)\chi P_n^{-\nu}(\chi) - (n+\nu) P_{n-1}^{-\nu}(\chi)] \times [n+1+\nu]^{-1}, \tag{A19}$$

where

$$P_0^0(\chi) = P_{-1}^0(\chi) = 1 \tag{A20a}$$

and

$$P_0^{-1}(\chi) = P_{-1}^{-1}(\chi) = [(1-\chi)/(1+\chi)]^{1/2} \tag{A20b}$$

can be used to start the recursions.

Geometrically, (A18) means that Eq. (A17) converges in the region of the (r, z) plane outside the semicircles

$$r^2 = z^2 + R_2^2 \tag{A21}$$

bounded below by the z axis and centered at the outer boundaries of the solenoid. Figure 1 shows the region in the (r, z) plane where neither (A1) nor (A17) will

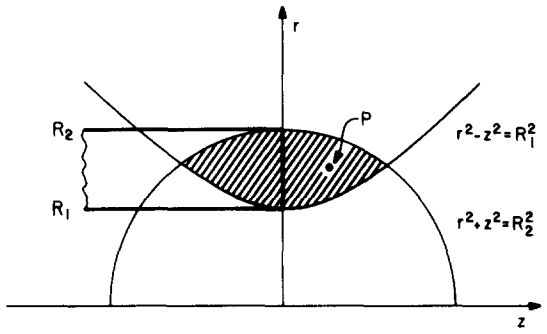

FIG. 1. Region of nonconvergence for two expansions. Points in the shaded area cannot be calculated using either (A1) or (A17).

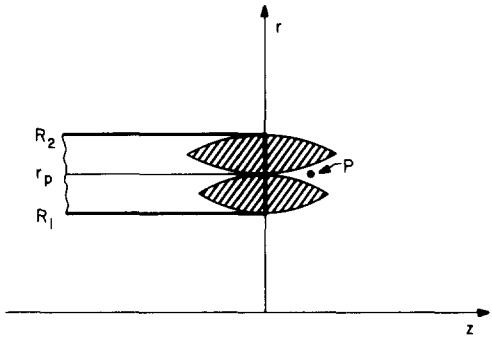

FIG. 2. Partition of solenoid winding for convergence. Point P in Fig. 1 defines a partition of the solenoid winding into two parts in such a way that the calculation converges at P. The shaded region of nonconvergence now does not include P.

converge. A point P in the shaded area cannot be calculated using only the series in (A1) or the series in (A17).

It is possible to calculate the field at the point P in Fig. 1 by dividing the solenoid into two sections, as in Fig. 2. Dividing the solenoid winding into parts with $r > r_p$ and $r \leqslant r_p$, (A17) can be applied to calculate the field due to the lower part while (A1) can be applied to calculate the field due to the upper part. In this way the field can be calculated at any point in the (r, z) plane with assurance that the series being summed is convergent. Economical achieving this convergence numerically is possible in practice using the information given above.

ACKNOWLEDGMENTS

This work was supported by the U.S. Department of Energy under contract with the University of California (Contract No. W7405-ENG-36).

REFERENCES

1. M. W. GARRETT, *J. Appl. Phys.* **22** (1951), 1091.
2. G. V. BROWN AND L. FLAX, *J. Appl. Phys.* **35** (1964), 1764.
3. J. R. MERRILL, *Rev. Sci. Instr.* **41** (1970), 1849.
4. V. I. DANILOV AND M. IANOVICI, *Nucl. Instr. Methods* **94** (1971), 541.
5. B. MONTGOMERY, "Solenoid Magnet Design," Wiley–Interscience, New York, 1969.
6. F. BOWMAN, "Introduction to Bessel Functions," Dover, New York, 1958.
7. M. ABROMOWITZ AND I. STEGUN, "Handbook of Mathematical Functions," National Bureau of Standards, Washington, D.C., 4th Printing, with Corrections, December 1965.
8. G. N. WATSON, "A Treatise on the Theory of Bessel Functions," Cambridge Univ. Press, Cambridge, Mass., 1966.
9. V. K. ZWORYKIN *et al.*, "Electron Optics and the Electron Microscope," Wiley, New York, 1945.
10. I. N. SNEDDON, "Special Functions of Mathematical Physics and Chemistry," Interscience, New York, 1961.